Proceedings of the Seventh International Conference on
Railway Technology: Research, Development and Maintenance
Edited by: J. Pombo
Civil-Comp Conferences, Volume 15, Paper 10.15
Civil-Comp Press, Edinburgh, United Kingdom, 2026
ISSN: 2753-3239, doi: 10.4203/ccc.15.10.15

Experimental Investigation of the Correlation Between Contact Wire Gradient and Pantograph Accelerations

B. V. Chennoju[1], M. Carnevale[2], C. E. A. Reyes[1], A. Collina[1] and S. Bruni[1]

[1] Department of Mechanical Engineering, Politecnico di Milano, Italy
[2] Department of Ingegneria Industriale e dell'Informazione, University of Pavia, Italy

Abstract

Condition assessment of overhead contact line (OCL) systems in electrified railways is traditionally based on geometric measurements such as contact wire height, gradient and stagger obtained from diagnostic vehicles. However, geometric measurements alone provide only a partial description of the dynamic quality of pantograph–OCL interaction. This paper investigates the relationship between OCL geometry and pantograph dynamic response using geo referenced measurements from in service trains and diagnostic vehicles. Pantograph accelerations are analysed using RMS indicators evaluated over 1 km spatial windows and short time windows of 200 ms. The OCL geometry is described using contact wire height and 5 m gradient with a sampling interval of 25 cm. The comparison is performed by spatially aligning the geometric and dynamic indicators and analysing their correspondence in different frequency bands. The results suggest that the contact wire gradient contributes to the pantograph acceleration response. However, a clear local correspondence between gradient and acceleration is observed only in selected regions, indicating that other infrastructure factors also influence the pantograph response. These findings show that pantograph

based dynamic indicators can complement OCL measurements in the assessment of OCL condition.

Keywords: Pcondition monitoring, high speed train, pantograph-catenary dynamic characteristics, pantograph–overhead contact line, pantograph, overhead contact system

1 Introduction

Electrified railways rely on continuous sliding contact between a pantograph and the overhead contact line (OCL) to ensure stable traction power supply to the trains. In current industrial practice, condition assessment of the OCL is still strongly shaped by periodic inspection workflows. In particular, key geometric parameters such as contact wire height and stagger are commonly obtained from inspection vehicles. Recent reviews summarize that these geometry-detection systems use lasers, image acquisition and image processing modules [1, 2]. These measurements often require compensation techniques to mitigate the influence of vehicle vibration and measurement noise. Previous work by the authors developed onboard diagnostic processing and geo-localisation methods for rolling-stock based monitoring, enabling pantograph acceleration indicators to be associated with their actual position along the railway line and compared across repeated runs [3,4]. In particular, the geo-localisation framework demonstrated that repeatable diagnostic indicators can be obtained from measurements, providing the basis for automated spatial comparison and trend analysis [5]. The present study builds on this framework by comparing geo-localised pantograph dynamic indicators with OCL geometry measurements, with the specific aim of assessing whether contact wire geometry alone can explain the observed pantograph response.

Experimental and simulation studies demonstrate that contact wire irregularities affect current collection and pantograph dynamics, but the resulting interaction signatures also depend on operating conditions and defect type [6, 7]. Therefore, prior work has investigated dynamic sensing strategies that use pantograph acceleration as a practical indicator of interaction quality and infrastructure condition. In this context, acceleration-driven monitoring frameworks have been proposed to compute condition indicators during operation and compare them with alarm thresholds, supporting condition-based maintenance concepts [3]. Field-deployed monitoring studies further emphasise the need for validation under service conditions and repeatability assessment beyond single-run testing [8]. Related developments in railway track condition monitoring have shown that in-service vehicles equipped with acceleration sensors and positioning systems can be used to estimate track irregularities, detect localised defects and increase the frequency of condition assessment [9, 10].

This paper investigates the use of geo referenced pantograph acceleration data acquired by in service trains and contact wire geometry data acquired by diagnostic trains. The pantograph acceleration data from in service train include RMS values acquired over 1 km spatial windows and short time windows of 200 ms, computed every 20 ms with 90% overlap between consecutive windows. The OCL geometry measurements by the diagnostic trains include contact wire height and 5 m gradient at a spatial sampling interval of 25 cm. Based on these data, the correlation between pantograph acceleration and contact wire gradient is analysed to assess whether or not the variations in the contact wire profile are reflected in the pantograph dynamic response. The main aspects of this relation are presented and discussed in the following subsections.

2 Line measurements for monitoring

The data collection from a number of in-service trains operating on high speed lines is performed. In this paper, the dataset from two high speed lines referred to as High speed line 1 and High speed line 2 is presented. It is worth noting that the data are continuously acquired onboard, geo-referenced and automatically transmitted to remote servers enabling large-scale aggregation and systematic analysis across multiple runs.

2.1 Pantograph acceleration measurements

Pantograph dynamic behaviour is quantified using acceleration RMS indicators that are acquired by the onboard data acquisition system. The dataset includes RMS values of accelerations evaluated over 1 km spatial windows (RMS–1km), RMS values evaluated over 200 ms time windows (RMS–SW), train speed and the corresponding progressive kilometric position (PK) along the track. The pantograph consists of two collector heads, with Sensor 1 and Sensor 2 mounted on different collectors at opposite lateral ends.

2.1.1 1 km window RMS

The RMS–1km indicator provides a spatially averaged description of the pantograph dynamic response along the line and is used to identify sections where the response remains high over relatively long distances. For the RMS–1km indicator, four frequency bands are facilitated namely, Band 1, Band 2, Band 3 and Band 4. Band 1 corresponds to 0–5 Hz frequency range that represents long wavelength excitation mechanisms such as span-passing dynamics. Band 2 corresponds to 5–30 Hz frequency range for shorter wavelength effects such as dropper-passing excitation. Band 3 corresponds to 150–185 Hz frequency range to capture flexural modes of vibration of the collector heads, mainly excited by the occurrence of impacts during operation. Band 4 corresponds to 0–180 Hz frequency range for broadband acceleration level. Figure 1 reports the RMS–1km values for the High speed line 1 and High speed line 2, together with the corresponding operated train speed. The results are shown for both pantograph sensors and for the same train running on different days in March 2026.

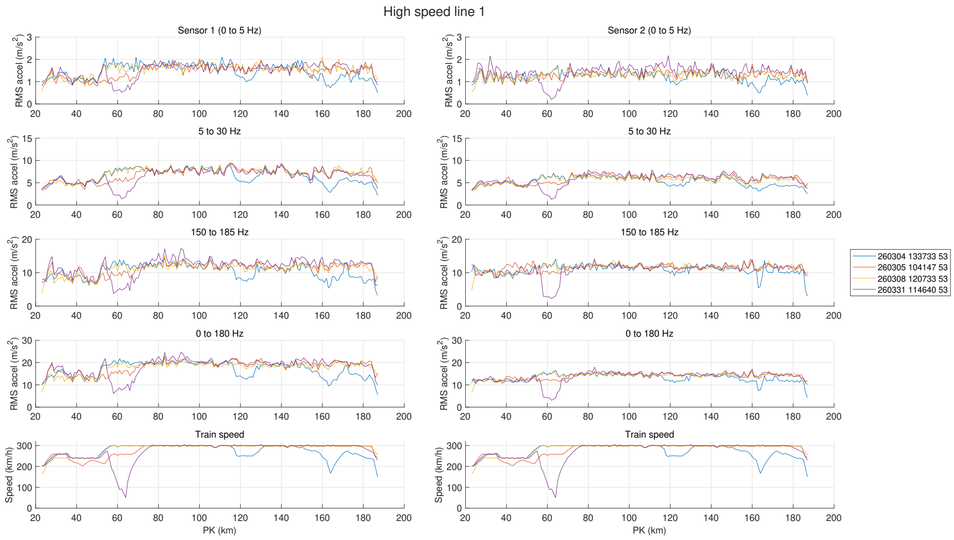

(a) High speed line 1

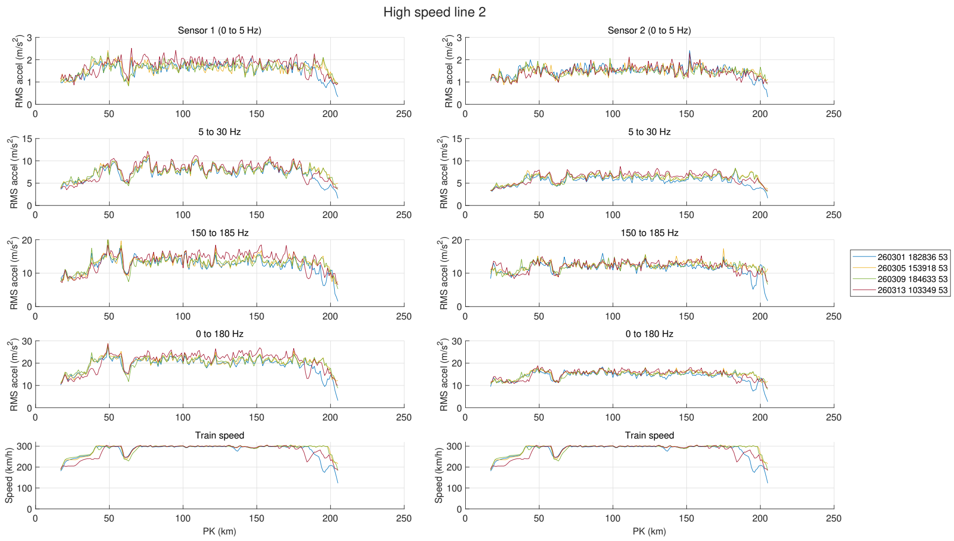

(b) High speed line 2

Figure 1: Pantograph acceleration RMS over 1 km windows.

The results show a repeatable spatial pattern across different runs. Although the RMS level is influenced by train speed, sections travelled at comparable speeds show similar trends. This is particularly visible in the 80–110 km region, where the train reaches approximately 300 km/h in the runs considered. It is important to note that the acceleration activity of Sensor 1 is different compared to Sensor 2, due to the left/right asymmetry of the collector constraints to the upper frame. The reference pantograph head has indeed a tie constraint on one side, and an hinge on the other side.

2.1.2 Short window RMS

The RMS–SW measurements provide a more detailed variation of the pantograph acceleration in 200 ms window with a sampling frequency of 20 ms with 90% overlap among the subsequent windows. The RMS–SW, including frequency content up to 250 Hz, can be exploited as an indicator of impact occurring on the collectors along the line, generated by singular points, which might correspond to local defectiveness. The peaks that are averaged in the 1 km window RMS are more clearly visible with the short window representation. To keep the results readable, Figure 2 shows one representative run for each of the two considered routes.

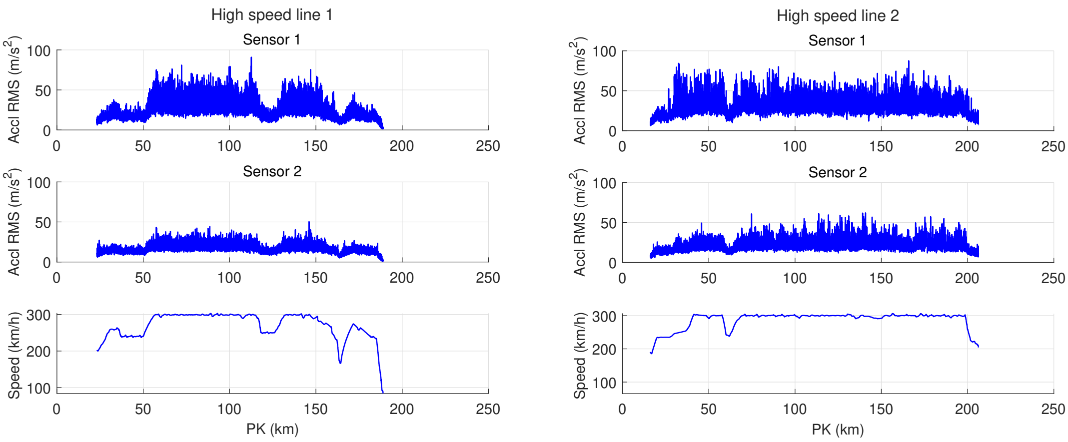

(a) High speed line 1 (b) High speed line 2

Figure 2: Pantograph acceleration RMS over short windows.

Similarly, the repeatability of the RMS–SW indicator is assessed for both lines by comparing several runs in the high speed operating region. A zoomed view showing the repeatability within a 1 km window is presented in Figure 3.

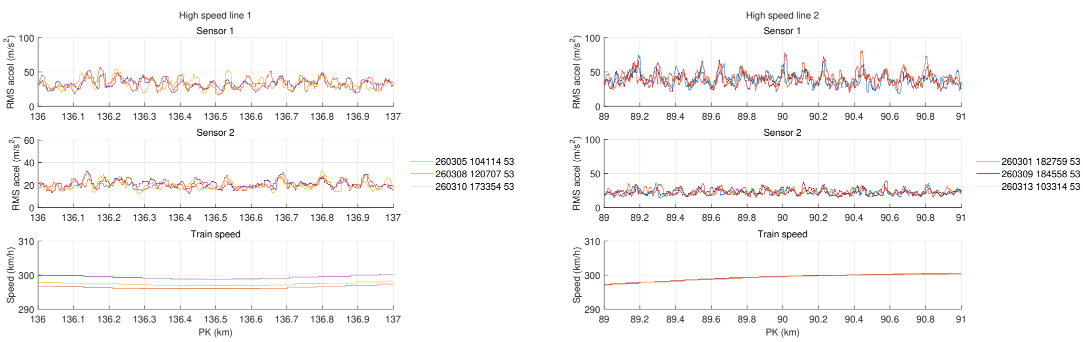

(a) High speed line 1 (b) High speed line 2

Figure 3: Repeatability of RMS–SW for both sensors.

The repeatability comparison shows that the main peaks occur at similar PK locations in different runs for both routes and both sensors. This indicates that the RMS–SW indicator can identify locations where the pantograph dynamic response is repeatedly high along specific spans of the OCL. However, the amplitudes of the oscillations vary between runs because the operating environment and contact conditions may change from one passage to another. Therefore, potential defective locations can be assessed more robustly by verifying whether high RMS–SW peaks recur at the same PK locations over multiple repeated runs.

2.2 OCL geometry measurements

The OCL geometry is measured by a diagnostic train and characterised using geo referenced measurements of the contact wire height, lateral stagger and longitudinal position along the track. These measurements allow the OCL geometry to be represented in the spatial domain and aligned with the fleet based pantograph acceleration measurements. In the considered high speed lines, the contact wire has no sag in the static configuration. In overlap regions between adjacent OCL sections, where two contact wires are present, the heights of both wires are recorded. The effective height is therefore defined as the minimum of the two measured contact wire heights. The spatial sampling interval associated with the progressive kilometric position is 25 cm, which limits the reliable spatial frequency content to approximately 166 Hz at 300 km/h according to the Nyquist criterion.

The relation between absolute height based statistics and the pantograph acceleration RMS is first evaluated. However, this comparison does not show a clear relationship, indicating that the absolute contact wire height alone is not sufficient to describe the local dynamic response of the pantograph. Therefore, the analysis is extended to the spatial variation of the contact wire height through gradient based indicators. Two gradient indicators are considered as shown in Figure 4. The first is the raw gradient, derived from the effective contact wire height as the spatial derivative with respect to distance. The second is the 5 m gradient measured by the diagnostic train, which represents the variation of the effective contact wire height over a fixed 5 m spatial baseline and is expressed as,

$$G_{5m}(s) = \frac{h(s+5) - h(s)}{5},$$

where $h(s)$ is the effective contact wire height at the progressive distance (s). Since the height is expressed in mm and the spatial baseline is expressed in m, the 5 m gradient is expressed in mm/m. Compared with the pointwise raw gradient, the 5 m gradient provides a finite baseline description of the contact wire slope and is less sensitive to local noise and sampling irregularities.

The raw gradient contains stronger short wavelength components and is therefore more sensitive to local geometric irregularities. In contrast, the 5 m gradient smooths these local fluctuations and provides a filtered description of the contact wire height variation over a finite spatial baseline, while retaining the dominant span passing com-

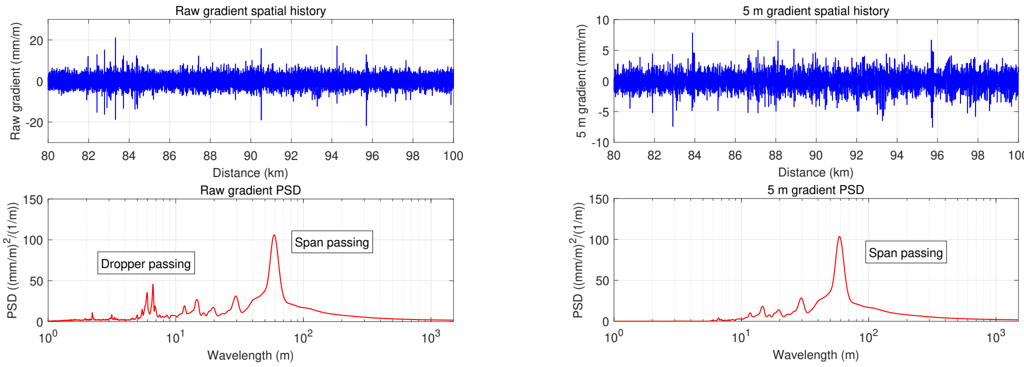

Figure 4: Spatial history and power spectral density of the raw and 5 m gradients of the contact wire.

ponent. Since both indicators are sampled at 25 cm, their differences arise from the way the gradient is defined rather than from the spatial resolution. These two indicators therefore describe complementary aspects of the contact wire geometry and are subsequently compared with the pantograph acceleration RMS evaluated over 1 km spatial windows and 200 ms short time windows to assess how gradient variations influence the measured pantograph dynamic response.

3 Investigation of the relation between contact wire gradient and pantograph acceleration

In this section, a case study based on High speed line 1 data is presented to investigate the relationship between the OCL gradient and pantograph acceleration using the RMS–1km and RMS–SW indicators. Due to space limitations, the High speed line 2 results are omitted without loss of the intended conclusions. As mentioned previously in Section 2, the pantograph is instrumented with two sensors, namely Sensor 1 and Sensor 2. To account for the response of both collectors, their contributions are also combined using the root sum square of the RMS values,

$$\mathrm{RMS_{comb}} = \sqrt{\mathrm{RMS}_1^2 + \mathrm{RMS}_2^2}.$$

where, RMS_1 and RMS_2 are the RMS values of Sensor 1 and Sensor 2 respectively.

3.1 1-km window analysis

The combined acceleration RMS is compared with the standard deviation of the OCL gradient. Since the acceleration RMS is evaluated in different frequency bands, the gradient is filtered into corresponding bands by converting the spatial history into an equivalent time history, assuming a constant train speed of 300 km/h. The comparison is therefore restricted to the high speed region where the train speed remains close to this value, for example between 80 and 105 km for the High speed line 1 case, as shown in Figure 1a. For the lower frequency bands, the acceleration and gradient comparisons are directly consistent. However, the 150–185 Hz and 0–180 Hz acceleration bands should be interpreted considering the bandwidth limitation of the OCL geometry measurements. In these cases, the gradient metric represents the full available gradient content rather than exactly the same frequency interval. Since repeated runs on different days showed good repeatability, one representative run is selected for the detailed analysis.

Figure 5 compares the combined acceleration RMS ($\mathrm{RMS}_{\mathrm{comb}}$) with the band wise standard deviation of the raw gradient over 1 km windows. The acceleration response is shown on the left vertical axis, while the gradient STD is shown on the right vertical axis. The full 80 to 105 km region is shown in Figure 5a, and a zoomed 7 km region is shown in Figure 5b.

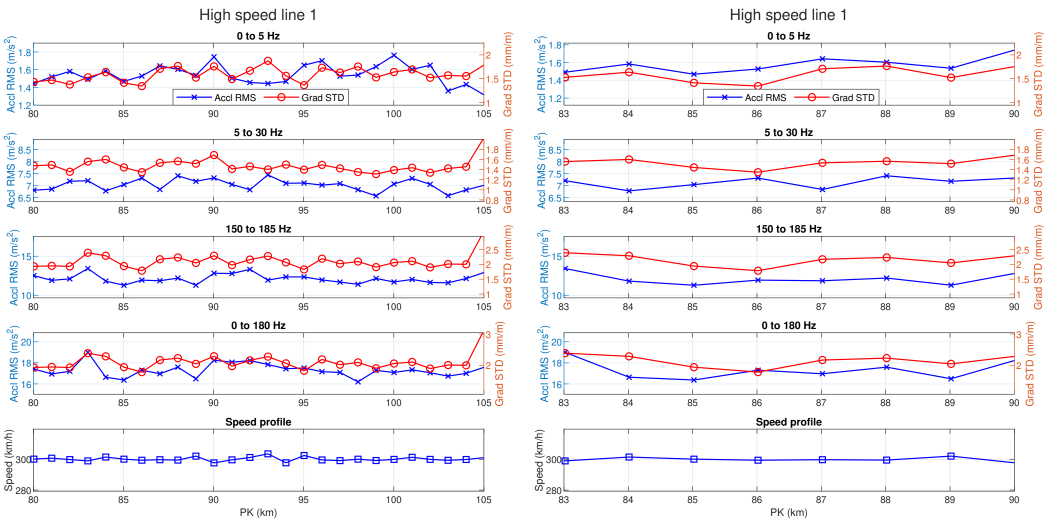

(a) 80-105 km region.

(b) Zoomed for 7 km.

Figure 5: Spatial comparison between the combined acceleration RMS and the band wise raw gradient STD along the high speed line 1.

In the 0–5 Hz band, a partial spatial correspondence is observed between the combined acceleration RMS and the gradient STD, particularly in the zoomed region. This suggests that the low frequency pantograph response is influenced by long wavelength variations of the contact wire geometry. However, the relation is not strictly proportional over the complete section, since some local variations in the gradient STD are not reproduced with the same intensity in the acceleration RMS and vice versa. In the 5–30 Hz band, the correspondence becomes less evident, although this band may still include shorter wavelength geometric variations and dropper related effects. For the 150–185 Hz band and the overall 0–180 Hz band, the comparison must be interpreted with caution. The gradient signal is limited to approximately 160 Hz due to the 25 cm spatial sampling interval, and the raw gradient is also more sensitive to measurement noise. Consequently, the weaker correspondence observed in these bands cannot be attributed only to the absence of a physical relation between contact wire geometry and pantograph acceleration. It may also reflect the bandwidth limitation of the available gradient signal and the noise amplification introduced by differentiation.

3.2 Short window analysis

Since the 1 km window analysis showed a partial correspondence between the raw gradient STD and the acceleration RMS in the 0 to 5 Hz band over selected regions, the short window analysis is focused on the longer wavelength component of the contact wire vertical profile. For this purpose, the 5 m gradient was utilized instead of the raw numerical gradient, since it provides a smoother representation of the height variation and reduces the influence of very short wavelength fluctuations and measurement noise. The maximum value of the 5 m gradient was then evaluated within a 16 m spatial window and compared with the short window acceleration RMS (since the short window length of 200 ms correspond to 16 m at 300 km/h). This representation provides a more local description of the contact wire gradient observing the peaks and also the larger wavelength features. Figure 6 shows the comparison between the combined RMS ($\mathrm{RMS}_{\mathrm{comb}}$) and the maximum 5 m gradient in each 16 m window. The corresponding stagger pattern is also shown for two representative regions. The stagger profile is included to indicate the lateral position of the contact wire and the associated support locations along the line. In addition, the shape of the stagger pattern provides information on the track alignment, since a nearly linear stagger variation is generally associated with straight track sections, whereas a curved stagger pattern may indicate curved track conditions. This representation allows the acceleration RMS, the vertical height based gradient indicator and the stagger pattern to be examined over the same spatial interval.

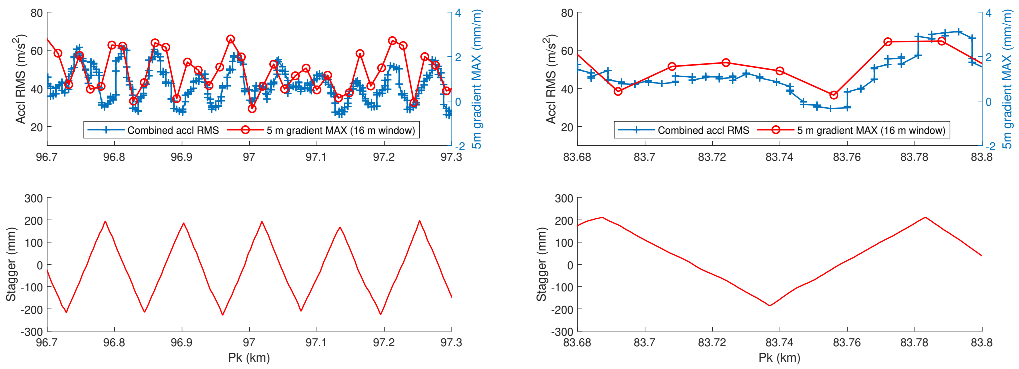

(a) First region. (b) Second region.

Figure 6: Short window comparison in two regions with spatial correspondence.

A clearer correspondence can be observed between the two quantities in Figure 6. In both regions, several local increases and decreases in the maximum 5 m gradient are accompanied by similar variations in the acceleration RMS. This behaviour is particularly relevant because the acceleration RMS exhibits periodic spatial undulations that are consistent with span passing effects. The comparison suggests that large wavelength variation of the contact wire vertical profile directly contributes to the low frequency acceleration response. However while this is observed, it is important to note that the pantograph response can also be influenced by its own structural dynamics and by other characteristics of the OCL system that are not fully represented by the vertical height of the contact wire. To support this this claim, the same comparison was then repeated over other regions to assess whether the observed relation was consistent. Figure 7 shows a representative case with higher acceleration activity region with similar gradient fluctuation levels with stagger pattern.

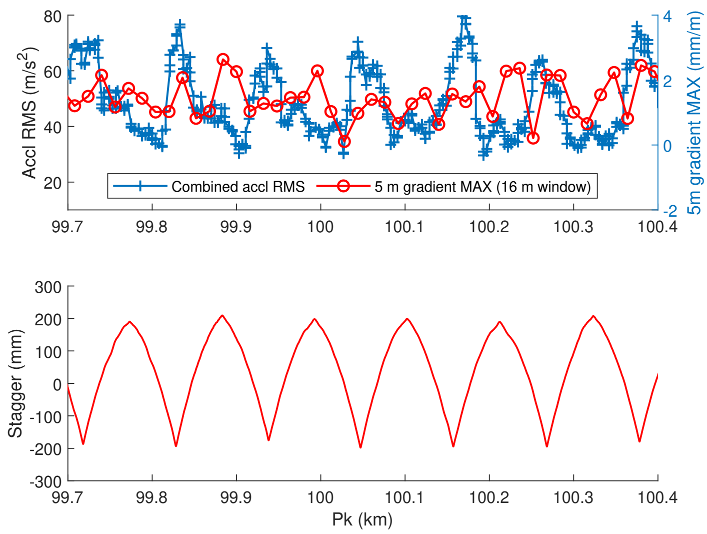

Figure 7: Short window comparison with weak spatial correspondence.

Although some local peaks in the gradient are accompanied by variations in the acceleration RMS, several acceleration peaks occur without a corresponding increase in the gradient indicator, for example between 99.8 km and 100.2 km. This indicates that the OCL gradient alone is not sufficient to explain the observed acceleration peaks across different operating conditions. In this region, the stagger pattern is slightly curved, which suggests the presence of curved track conditions. Therefore, the pantograph dynamic response may also be influenced by excitation mechanisms other than the vertical contact wire profile. These may include support related effects associated with the stagger pattern of the OCL and possible track related inputs. Such effects are not fully captured by the vertical height based OCL features considered in the present analysis.

4 Conclusions

This paper investigated the relation between OCL geometry and pantograph dynamic response using geo referenced measurements from high speed railway operation. Pantograph acceleration measurements are used as dynamic indicators of the pantograph and OCL interaction, while contact wire height measurements are used to describe the vertical height and gradient of the contact wire.

The measurement framework was first introduced by describing the available line measurements of OCL and the corresponding operated pantograph's acceleration data. The pantograph response was evaluated using RMS based indicators over both spatial 1 km windows and shorter time windows T=0.2 sec. The 1 km RMS was used to describe the spatial evolution of the response over long sections (approximately corresponding to the length of a contact wire section between two section overlaps), while the short window RMS was used to examine the dynamic effects related to local impacts. In the 1 km window analysis, the raw gradient STD was compared with the acceleration RMS in different frequency bands. A partial correspondence was observed in the 0 to 5 Hz band over a few regions, suggesting that pantograph acceleration response can be used as a quantitative indicator of long wavelength variations of the contact wire vertical profile. However, the relation between STD of acceleration and contact wire gradient was not strictly proportional over the complete section of the OCL, leading to a correlation index between the two quantities insufficient for the development of a predictive model capable of estimating the contact wire gradient based on accelerations.

Based on this observation, the short window analysis was refined using the 5 m gradient. The 5-m gradient maxima, evaluated within a 16 m window, showed clearer spatial correspondence with the short window acceleration RMS in straight line. However, the same behaviour was not observed consistently across curve sections. In these regions, further investigation should be carried out, evaluation the extension of the compact 2-sensors setup, exploited in this work to contain the costs of the commercial-service diagnostic system.

Overall, the presented result confirm that the geometry of the contact wire represents only one of the mechanisms influencing the pantograph response. In the high-speed case considered, and with the 2-sensors pantograph setup, the acceleration response can not be directly exploited as a 1:1 indicator to reconstruct c.w. vertical profile.

References

[1] Jose A. Sainz-Aja, Joao Pombo, Jordan Brant, Pedro Antunes, Jose M. Rebelo, Jose Santos, and Diego Ferreno. Real-time rail electrification systems monitoring: A review of technologies. *Sensors*, 25:6625, 2025.

[2] Wei Zhou, Zhe Qin, Xinyu Du, Xiantang Xue, Haiying Wang, Hailang Li, et al. Measurement method for contact wire wear based on stereovision. *Sensors*,

24(7):2085, 2024.

[3] Marco Carnevale and Andrea Collina. Processing of collector acceleration data for condition-based monitoring of overhead lines. *Proceedings of the Institution of Mechanical Engineers, Part F: Journal of Rail and Rapid Transit*, 230(2), 2016. First published online 2014.

[4] M Carnevale, I La Paglia, and P Pennacchi. An algorithm for precise localization of measurements in rolling stock-based diagnostic systems. *Proceedings of the Institution of Mechanical Engineers, Part F: Journal of Rail and Rapid Transit*, 235(7):827–839, 2021.

[5] Marco Carnevale, Andrea Collina, Marco Palmiotto, et al. Condition monitoring of railway overhead lines: Correlation between geometrical parameters and performance parameters. In *Proceedings of the First World Congress on Condition Monitoring (WCCM 2017)*, pages 1–11, 2017.

[6] Andrea Collina, Fabio Fossati, Marco Papi, and Ferruccio Resta. Impact of overhead line irregularity on current collection and diagnostics based on the measurement of pantograph dynamics. *Proceedings of the Institution of Mechanical Engineers, Part F: Journal of Rail and Rapid Transit*, 221(4):547–559, 2007.

[7] Sam Hayes, David I. Fletcher, Adam E. Beagles, and Katherine Chan. Effect of contact wire gradient on the dynamic performance of the catenary pantograph system. *Vehicle System Dynamics*, 59(12):1916–1939, 2021.

[8] Borja Rodriguez-Arana, Pablo Ciaurriz, Nere Gil-Negrete, and Unai Alvarado. A non-intrusive monitoring system on train pantographs for the maintenance of overhead contact lines. *Sensors*, 23(18):7890, 2023.

[9] Hirotaka Mori, Hitoshi Tsunashima, Takashi Kojima, Akira Matsumoto, and Takeshi Mizuma. Condition monitoring of railway track using in-service vehicle. *Journal of Mechanical Systems for Transportation and Logistics*, 3(1):154–165, 2010.

[10] Xiukun Wei, Feng Liu, and Limin Jia. Urban rail track condition monitoring based on in-service vehicle acceleration measurements. *Measurement*, 80:217–228, 2016.